Supporting Information

Pulsed EPR spectra. We also obtained the temperature dependence of the pulsed EPR (Bruker ESP 380E) spectra for the DQ-TMB system in DMF as shown in figure S1. Well-resolved spectra confirm the origin of the temperature effect on the S-T_0 RPM phases.

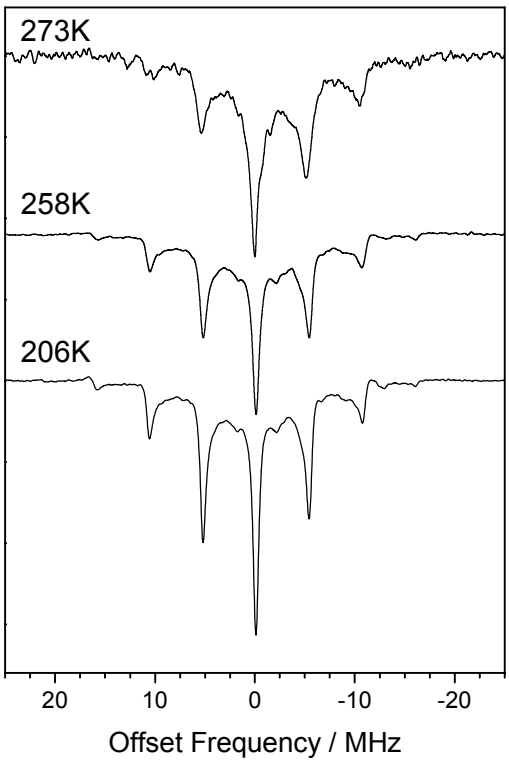

Figure S1. Temperature dependence of the echo detected FT-EPR spectra observed at 200 ns after the 355 nm laser excitations in the DQ-TMB system in DMF around the g-center fields of the duroquinone anion radicals.

Cyclic Voltammetry. Temperature dependence of the reduction and oxidation potentials of DQ and TMB was respectively measured by the cyclic voltammetry (Model P-1000, YANACO) under the deaerated conditions in DMF and BuN. Tetra-*n*-propylammonium perchlorate (0.1 M) was used as the supporting electrolyte. The working and counter electrodes were platinum, while the reference was standard calomel electrode. A nitrogen flow cryostat was used to control the temperature. Schematic cell configuration is shown in Figure S1. The temperature was monitored in the sample solution at the working and counter electrodes. The reference electrode was under room temperature. The reduction and oxidation potentials were obtained under the same experimental setup. The potentials in Table 1 may be different from the values under the isothermal cell condition. However, the energy gap obtained by $-\Delta G_{CR} = E_{1/2}^{ox} - E_{1/2}^{red}$ can be treated as the value at the temperature of the working and counter electrodes, since the effect of the temperature difference in the reference electrodes is subtracted.

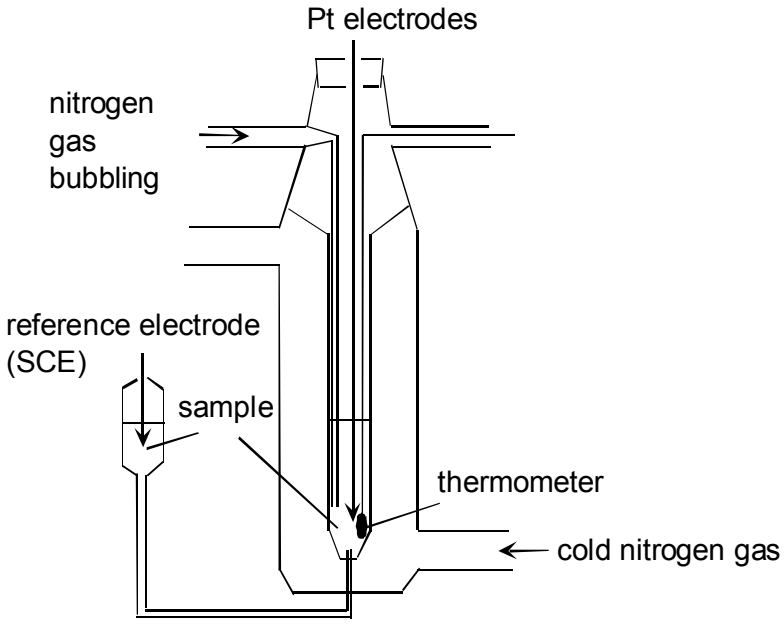

Figure S2. Schematic cell configuration for the CV measurement.

Singlet-Triplet Energy Splitting (J_{CT}) in RIP. According to the charge-transfer interaction mechanism,[7] the J_{CT} is formulated as follows,

$$J_{\mathrm{CT}}(r)=\sqrt{\frac{\lambda_{\mathrm{S}}(r)}{2\pi k_{\mathrm{B}}T}}V(r)^2\sum_{j_{\mathrm{A}},j_{\mathrm{D}}}FC(j_{\mathrm{A}})FC(j_{\mathrm{D}})\int_{-\infty}^{\infty}\frac{\exp\left\{-\frac{\lambda_{\mathrm{S}}(r)}{2k_{\mathrm{B}}T}X^2\right\}dX}{\lambda_{\mathrm{S}}(r)(2X-1)-j_{\mathrm{D}}h\upsilon_{\mathrm{D}}-j_{\mathrm{A}}h\upsilon_{\mathrm{A}}+\Delta G_{\mathrm{CR}}}, \qquad \text{(S1)}$$

where

$$V(r)^2=V_0{}^2\exp\{-\beta(r-d)\}, \qquad \text{(S2)}$$

$$FC(j_{\mathrm{b}})=\exp(-S_{\mathrm{b}})\frac{S_{\mathrm{b}}{}^{j_{\mathrm{b}}}}{j_{\mathrm{b}}!}. \qquad \text{(S3)}$$

V_0 denotes the electronic coupling matrix element at the contact separation d,[15] and $FC(j_b)$ Franck-Condon factor between the vibrational wave functions in the neutral ground state and the ion radical in D or A molecule. X represents the normalized solvation coordinate. In eq S3, the high frequency ($h\upsilon_b$ = 1500 cm^{-1}) solute vibrational modes (b) of the C-O and C=O stretching were taken into account as the accepting modes associated with the intramolecular reorganizations of TMB and DQ accompanied by the CR process with the quantum number of j_b. The λ_V and υ_b are included in eq S3; $S_b = \lambda_V / h\upsilon_b$.

Analysis of RPM polarization. By using the Laplace-transform $\rho(r,s)$ of the density matrix of $r\rho(r,t)$ in the S-T_0 basis system, the magnitude of the RPM electron spin polarization (P_{RPM}) is numerically analyzed by the SLE as follows,

$$s\boldsymbol{\rho}(r,s) - r\boldsymbol{\rho}(r,t=0) = -i\left[\boldsymbol{H}_{\mathrm{RIP}}(r), \boldsymbol{\rho}(r,s)\right] + D\frac{\partial^2}{\partial r^2}\boldsymbol{\rho}(r,s) + \boldsymbol{K}\boldsymbol{\rho}(r,s), \tag{S4}$$

where the $\boldsymbol{H}_{\mathrm{RIP}}$ is the spin Hamiltonian composed of the Zeeman effect, hyperfine interaction and J_{CT}.[7] The $\boldsymbol{K}$ operator represents the r dependent CR reaction from the singlet RIP.[7] The solute diffusion coefficient was approximated by the Stokes-Einstein relation with using the solvent viscosity (η) and the radius (d_α) of the solute molecule as,

$$D_\alpha(T) = \frac{k_{\mathrm{B}}T}{6\pi\eta(T)d_\alpha}. \tag{S5}$$

The temperature dependence of η was assumed to be expressed with the Arrhenius form as,

$$\eta(T) = A \times \exp\left(-\frac{E_{\mathrm{a}}}{RT}\right). \tag{S6}$$

The A and E_{a} for DMF were estimated from ref 12; $A = 2.76\times10^{-5}$ Pa·s and $E_{\mathrm{a}} = 8555$ J mol^{-1} for DMF. Solute molecular sizes were described in ref 13. The D values obtained from eqs S5 and S6 were 1.1×10^{-5} cm^{2}s^{-1} at 285 K, 6.4×10^{-6} cm^{2}s^{-1} at 258 K and 4.5×10^{-6} cm^{2}s^{-1} at 236 K in DMF.

At lower temperature, the S-T_{-1} or S-T_{+1} RPM polarization may play a role. However, the magnitude of the electron spin polarization calculated by the S-T_{-1} or S-T_{+1} mechanism (for example, Adrian F.J.; *Chem. Phys. Lett*. **1994**, 229, 465.) was only ~0.01 P_{eq} with using the same diffusion coefficient and with the same hyperfine coupling as used in the P_{RPM} calculation in table 1 at 236 K. This result strongly supports that the S-T_0 RPM polarization dominates the intensity difference between the peaks in figure 1.